Anesthesiology 2005; 103:1156–66

Halothane Inhibition of Recombinant Cardiac L-type Ca^{2+} Channels Expressed in HEK-293 Cells

Kevin J. Gingrich, M.D., Son Tran, M.D.,† Igor M. Nikonorov, M.S.,‡ Thomas J. Blanck, M.D., Ph.D.§*

Background: **Volatile anesthetics depress cardiac contractility, which involves inhibition of cardiac L-type calcium channels. To explore the role of voltage-dependent inactivation, the authors analyzed halothane effects on recombinant cardiac L-type calcium channels ($\alpha_{1C}\beta_{2a}$ and $\alpha_{1C}\beta_{2a}\alpha_2/\delta_1$), which differ by the α_2/δ_1 subunit and consequently voltage-dependent inactivation.**

Methods: **HEK-293 cells were transiently cotransfected with complementary DNAs encoding α_{1C} tagged with green fluorescent protein and β_{2a}, with and without α_2/δ_1. Halothane effects on macroscopic barium currents were recorded using patch clamp methodology from cells expressing $\alpha_{1C}\beta_{2a}$ and $\alpha_{1C}\beta_{2a}\alpha_2/\delta_1$ as identified by fluorescence microscopy.**

Results: **Halothane inhibited peak current (I_{peak}) and enhanced apparent inactivation (reported by end pulse current amplitude of 300-ms depolarizations [I_{300}]) in a concentration-dependent manner in both channel types. α_2/δ_1 coexpression shifted relations leftward as reported by the 50% inhibitory concentration of I_{peak} and I_{300}/I_{peak} for $\alpha_{1C}\beta_{2a}$ (1.8 and 14.5 mM, respectively) and $\alpha_{1C}\beta_{2a}\alpha_2/\delta_1$ (0.74 and 1.36 mM, respectively). Halothane reduced transmembrane charge transfer primarily through I_{peak} depression and not by enhancement of macroscopic inactivation for both channels.**

Conclusions: **The results indicate that phenotypic features arising from α_2/δ_1 coexpression play a key role in halothane inhibition of cardiac L-type calcium channels. These features included marked effects on I_{peak} inhibition, which is the principal determinant of charge transfer reductions. I_{peak} depression arises primarily from transitions to nonactivatable states at resting membrane potentials. The findings point to the importance of halothane interactions with states present at resting membrane potential and discount the role of inactivation apparent in current time courses in determining transmembrane charge transfer.**

VOLATILE anesthetics (VAs) depress cardiac contractility by reducing cytosolic Ca^{2+} concentration through alteration of cellular mechanisms governing Ca^{2+} homeostasis. The critical first step in the increase of cytosolic Ca^{2+} in cardiac excitation–contraction coupling is the transmembrane entry of Ca^{2+} mediated by the opening of L-type Ca^{2+} channels (LCCs) triggered by membrane depolarization. The VA halothane is known to inhibit the entry of Ca^{2+} through the LCCs, which seems to be a primary effect by which halothane depresses cardiac contractility.[1–4]

Volatile anesthetics seem to depress LCC activity and subsequent Ca^{2+} entry by enhancing apparent channel inactivation.[5–10] However, drug block of open channels may also manifest as enhancement of apparent inactivation,[11] and recovery from drug-blocked states may mimic delayed recovery from inactivated states. Therefore, it is plausible that the apparent VA effects on inactivation may actually arise from a mechanism involving VA inhibition of open channels as reported in other examples of drug inhibition of ion channels.[11–13]

L-type Ca^{2+} channels are composed of multiple protein subunits (α, β, α_2/δ, and γ) where the α subunit contains the pore forming region.[14] The α subunit is composed of four domains, each with six transmembrane segments. Auxiliary β and α_2/δ subunits modulate the kinetics of channel opening as well as increase the number of functional channels expressed in heterologous expression systems such as *Xenopus* oocytes and human embryonic kidney cells (HEK-293). Channel inactivation is considered to have two distinct components that are each dependent on membrane voltage or Ca^{2+} influx.[15] Coexpression of the α_2/δ subunit enhances voltage-dependent inactivation of $\alpha\beta$ channels.[16,17]

The strategy of this study was to manipulate channel phenotype using recombinant channels of varying subunit composition. In addition, heterologous protein expression used small cells from mammalian cell lines that provided for high resolution analysis of current time courses. The objectives of this study were (1) to investigate the role of voltage-dependent inactivation in halothane inhibition of cardiac LCCs carried by recombinant $\alpha_{1C}\beta_2$ and $\alpha_{1C}\beta_2\alpha_2/\delta_1$ channels and (2) to determine the effects of halothane on the time course of the voltage-triggered activity in recombinant channels expressed in HEK-293 cells. Notably, this study is the first to investigate VA effects on recombinant LCCs expressed in a human cell line. Coexpression of α_2/δ_1 subunit with $\alpha_{1C}\beta_{2a}$ ($Ca_V1.2$) resulted in enhanced inactivation of Ba^{2+} currents as previously described[16] and greater inactivation enhancement and inhibition of peak currents (I_{peak}). Time course analysis indicates that halothane accelerated activation kinetics in both channels unattended by significant changes in peak conductance. Halothane inhibition of I_{peak} arises from channel transitions to nonactivatable states occurring at resting membrane potentials or early in activation, and primarily governs reductions in $\alpha_{1C}\beta_{2a}\alpha_2/\delta_1$ transmembrane

* Associate Professor, ‡ Research Associate, § Professor, Department of Anesthesiology, New York University, School of Medicine. † Resident, Department of Anesthesiology, University of Rochester, School of Medicine. Current position: Anesthesiologist, Anesthesia Medical Group, Inc., Orange, California.

Received from the Departments of Anesthesiology, New York University, School of Medicine, New York, New York, and University of Rochester, School of Medicine, Rochester, New York. Submitted for publication February 9, 2005. Accepted for publication July 2, 2005. Support was provided solely from institutional and/or departmental sources.

Address correspondence and reprint requests to Dr. Gingrich: Department of Anesthesiology RR-605, New York University, School of Medicine, 550 First Avenue, New York, New York 10016. Address electronic mail to: kevin.gingrich@med.nyu.edu.

charge transfer thought to heavily influence depression of cardiac contractile state.

Materials and Methods

Molecular Biology

HEK-293 cells were transiently cotransfected by calcium phosphate precipitation[18] with complementary DNAs encoding α_{1C} tagged with green fluorescent protein on the N termini to serve as a reporter,[19] and rabbit heart β_{2a}, with and without rabbit skeletal muscle α_2/δ_1 subunits. Cells were initially cotransfected with α_{1C}, but this method yielded low transfection efficiencies (< 5%) leading to poor experimental efficiency. To facilitate the identification of cells expressing α_{1C}, transfections were conducted with α_{1C} tagged with green fluorescent protein. Cells expressing the fusion protein were identified using fluorescence microscopy. Transfection efficiencies remained low (< 5%), but experimental efficiency was markedly enhanced.

Electrophysiology

Whole cell barium currents were recorded at room temperature 2–3 days after transfection from individual cells expressing α_{1C} tagged with green fluorescent protein as identified by fluorescence microscopy. This study focused on halothane effects on voltage-dependent inactivation, and therefore, Ba^{2+} was used as the charge carrier because it weakly triggers calcium-dependent inactivation.[20] Cells were voltage clamped using the whole cell configuration of the patch clamp technique at room temperature. An Axopatch 200A amplifier (Axon Instruments, Union City, CA) was connected to an IBM-compatible computer running the Axobasic (Axon Instruments) environment and software of our own design. Bath solution contained 130 mM *N*-methyl-D-glucamine-aspartate, 1 mM $MgCl_2$, 10 mM glucose, 10 mM 4-aminopyridine, 10 mM HEPES, and 20 mM $BaCl_2$, pH 7.3–7.4 with 1 M *N*-methyl-D-glucamine-aspartate. Internal solution contained 140 mM *N*-methyl-D-glucamine-methanesulfonate, 5 mM EGTA, 1 mM $MgCl_2$, 4 mM Mg-adenosine triphosphate, and 5 mM HEPES, pH 7.2–7.3 with CsOH. Currents were sampled at 10 kHz and filtered at 2 kHz. Currents were measured (−70 mV to −80 mV holding potential) in the presence of halothane (0–5 mM), and leak and capacitive transients were subtracted by a P/8 protocol. Interstimulus intervals were greater than 15 s.

The cell being investigated was continuously superfused with solutions delivered by a local solution changer,[21] which involved a closed system constructed entirely of stainless steel, glass, polytetrafluoroethylene tubing, and glass syringes with a syringe pump. Currents were obtained in control, drug, control sequence, and data were included provided the bracketing peak control current was greater than 90% of initial control. Using the internal and external solutions as described, pipette resistances were 2–5 MΩ, which was compensated by greater than 60%. Time constant for charging membrane capacitance was approximately 0.6 ms. The VA agent halothane in a thymol-free preparation (Halocarbon, River Edge, NJ) was diluted from a saturated solution (17.5 mM) and dissolved in the bath solution before being loaded into the local solution changer.

Data Analysis

Curve fitting and statistical analysis was performed with ORIGIN software (OriginLab, Northampton, MA). The data are shown as mean ± SEM, unless otherwise stated.

The maximum channel conductance (G_{peak}) was calculated using

$$G_{peak} = I_{peak}/(V - V_{rev}), \quad (1)$$

where V is the voltage of the activating depolarization, I_{peak} is the current maximum during the activating depolarization, and V_{rev} is the reversal potential as estimated by extrapolating the quasi-linear portion of the current–voltage (I-V) relation near zero current at positive voltages.

Voltage dependence of activation was quantified by first relating peak G_{peak} normalized by maximum G_{peak} to the activating voltage, which was followed by a quantitative description of this relation using a two-state Boltzmann equation of the form

$$\text{Normalized } G_{peak} = 1/\{1 + \exp([V - V_{1/2}]/dx)\}, \quad (2)$$

where V is voltage, $V_{1/2}$ is the midpoint voltage, and dx is the slope factor.

To quantify the kinetics of activation and inactivation, both time courses were fit simultaneously with

$$I(t) = A \times \exp(-t/\tau_a) + B \times \exp(-t/\tau_b) + C \times \exp(-t/\tau_c), \quad (3)$$

where I(t) is the current magnitude at time t, and A, B, and C are coefficients of the exponential components with time constants τ_a, τ_b, and τ_c, respectively.

Concentration–inhibition relations were fit with a sigmoidal equation of the form

$$Y = 1/\{1 + (IC_{50}/[A]^n\}, \quad (4)$$

where y is the response variable, [A] is the halothane concentration, IC_{50} is the concentration at 50% inhibition from control, and n is the slope factor related to the Hill coefficient.

Transmembrane Charge Transfer Calculation

Transmembrane charge transfer (Q_T) was calculated by integrating the area under the current response from the time it crossed the baseline after the capacity transient to the end of the triggering depolarization (+10

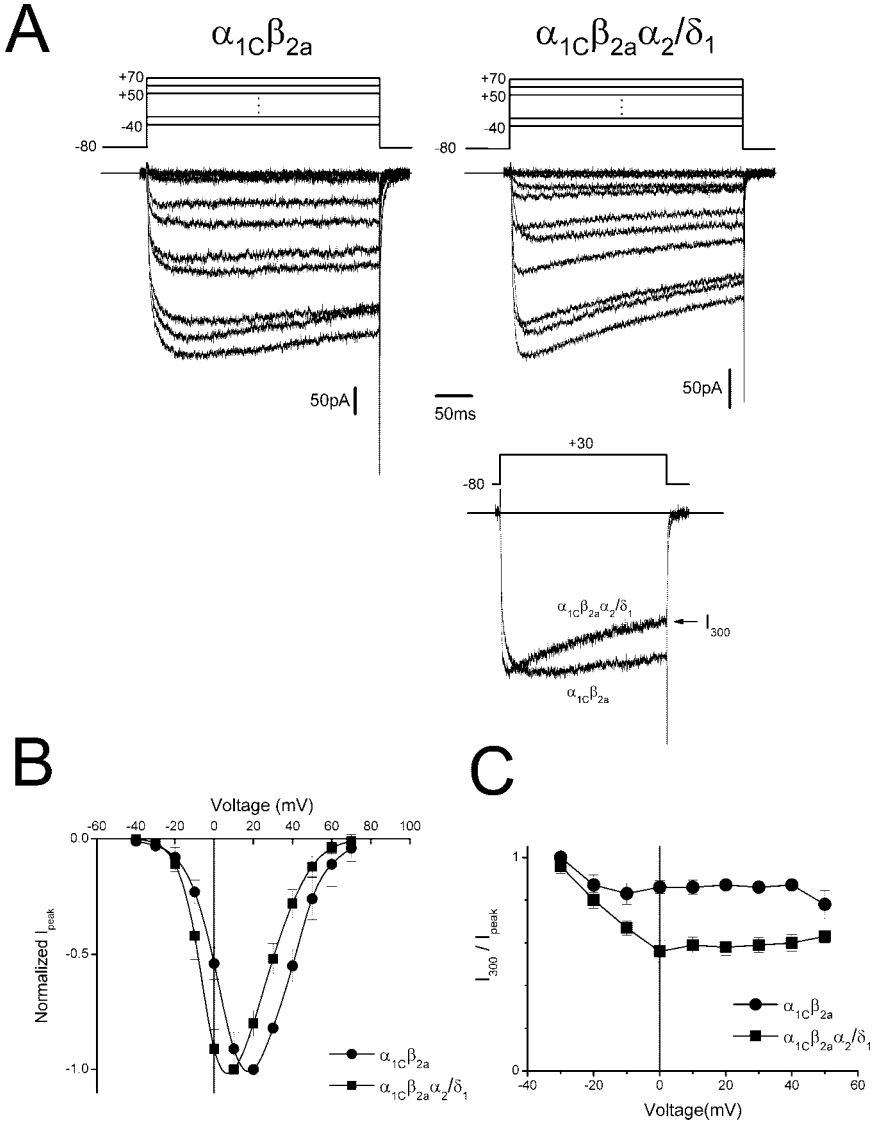

Fig. 1. Macroscopic Ba^{2+} currents from HEK-293 cells expressing $\alpha_{1C}\beta_{2a}$ and $\alpha_{1C}\beta_{2a}\alpha_2/\delta$ channels. (*A*) Representative current–voltage families triggered by voltage steps (−40 to +70 mV, 300 ms, 10-mV increments, holding potential −80 mV as drawn above) from single HEK-293 cells expressing $\alpha_{1C}\beta_{2a}$ or $\alpha_{1C}\beta_{2a}\alpha_2/\delta$ subunits as indicated. Current activation is marked by downward response deflection. *Inset* shows individual traces (+30 mV depolarization as drawn above) normalized to peak amplitude, replotted from current–voltage families for each channel as indicated to demonstrate differences in inactivation, which is reported by the current magnitude at the end of the 300-ms depolarization (I_{300}). (*B*) Current–voltage relations for indicated channels in grouped data. (*C*) Plots of fraction of current remaining at end of 300-ms depolarization (I_{300}) relative to peak current (I_{peak}) *versus* depolarizing voltage for both channels in grouped data. Inactivation by this measure is more than twofold greater for $\alpha_{1C}\beta_{2a}\alpha_2/\delta$ *versus* $\alpha_{1C}\beta_{2a}$ at voltages greater than −20 mV (see text). Grouped data are mean ± SEM (n = 4–6). Capacity and tail currents sometimes clipped for purposes of display.

mV, 300 ms). The relative contribution of I_{peak} changes were approximated by calculating fractional I_{peak} reduction relative to control. This approach determines Q_T occurring in the absence of alterations in current time course caused by changes in activation and inactivation kinetics. Reductions in Q_T that were unaccounted for by changes in I_{peak} were attributed to changes in gating kinetics reflected in alterations in current time course. Relative contributions of I_{peak} and kinetics were then calculated straightforwardly, assuming these two represented all contributing factors.

Results

Currents from Cells Transfected with $\alpha_{1C}\beta_{2a}$ or $\alpha_{1C}\beta_{2a}\alpha_2/\delta_1$ Subunits

Figure 1A shows a representative family of current responses triggered by a range of voltage steps from single HEK-293 cells transfected with either $\alpha_{1C}\beta_{2a}$ or $\alpha_{1C}\beta_{2a}\alpha_2/\delta_1$ subunits. The peak I-V relations (fig. 1B) show that maximum I_{peak} was evoked at approximately +20 mV for $\alpha_{1C\beta 2a}$ channels, whereas that for $\alpha_{1C}\beta_{2a}\alpha_2/\delta_1$ channels is leftward shifted by approximately 10 mV, consistent with previous reports.[16] Coexpression of α_2/δ_1 with $\alpha_{1C}\beta_{2a}$ subunits enhanced inactivation as reported by the current at the end of a single 300-ms depolarization (I_{300}; fig. 1A, inset) in single cells depolarized to +30 mV as well as in grouped data over a range of voltages (fig. 1C). These results indicate that voltage-dependent inactivation is potentiated by the presence of the α_2/δ_1 subunit in accord with previous reports[16,21] and that transfection resulted in the functional expression of LCCs with the expected subunit composition.

Halothane Depression of I_{peak} and Inactivation Enhancement Are Potentiated by α_2/δ_1 Coexpression

We next investigated the concentration dependence of halothane depression of I_{peak} and I_{300}. Currents trig-

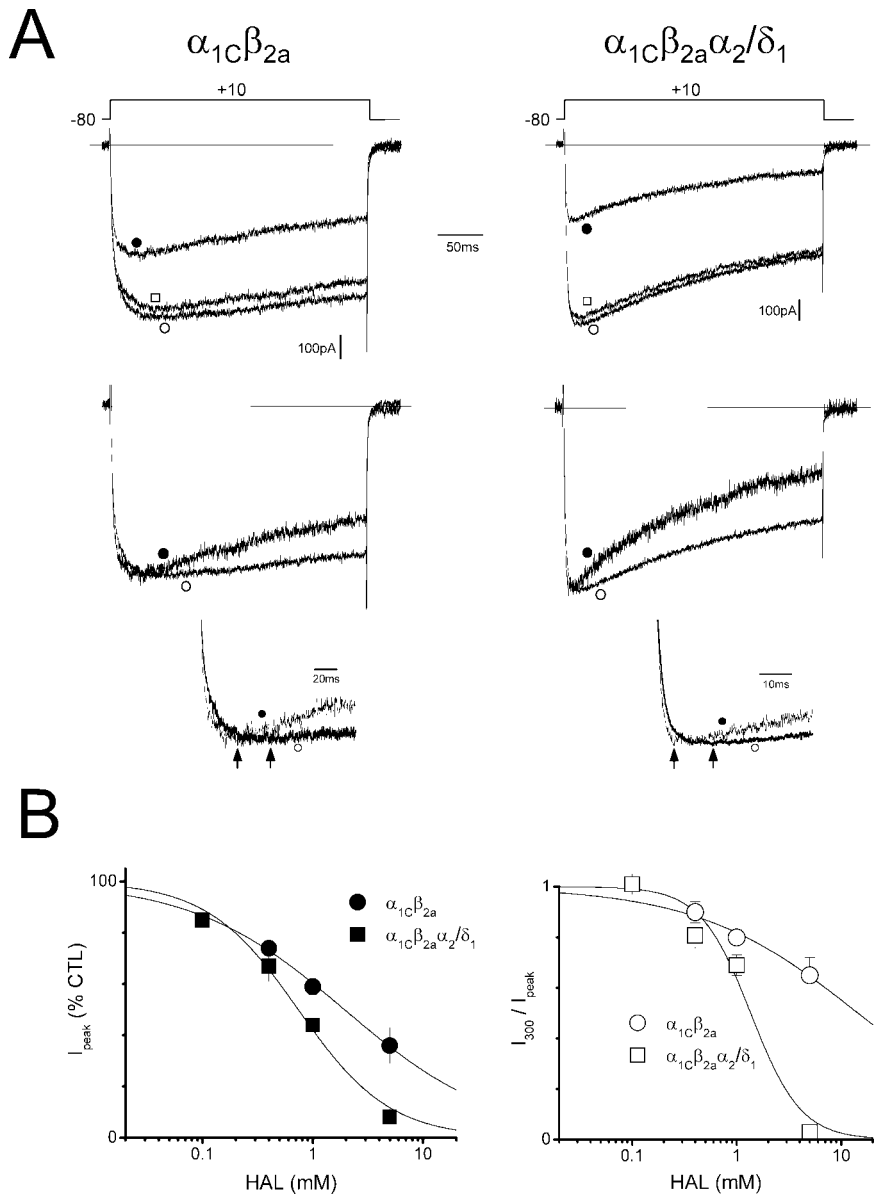

Fig. 2. Halothane effects on peak current, and inactivation of $\alpha_{1C}\beta_{2a}$ and $\alpha_{1C}\beta_{2a}\alpha_2/\delta_1$ channels. (*A*, *top*) Currents (+10 mV, 300 ms, holding = −80 mV as drawn above) recorded from individual HEK-293 cells expressing either $\alpha_{1C}\beta_{2a}$ (*left*) or $\alpha_{1C}\beta_{2a}\alpha_2/\delta_1$ (*right*) in control (○), 1 mM halothane (●), and after washout (□). *Solid horizontal lines* mark current baselines. (*A*, *bottom*) Responses in control (○) and 1 mM halothane (●) replotted from *A*, *top*, after normalization by peak current (I_{peak}) to provide for a comparison of the current time course. Tail currents sometimes clipped for purposes of display. (*Insets*) Responses from *A*, *bottom*, replotted on expanded timescale to show differences in time of I_{peak}, indicated by *arrows*, in control and 1 mM halothane for both channels. (*B*) Halothane (HAL) concentration–response relations for I_{peak} (*left*) and the current magnitude at the end of the 300-ms depolarization (I_{300}) (*right*) normalized to I_{peak} control (CTL) (I_{300}/I_{peak}) for each channel as indicated in grouped data (+10 mV, 300 ms, holding = −80 mV). *Solid lines* represent best fits of a logistic function (equation 4, see Materials and Methods) to I_{peak} and I_{300}/I_{peak} responses for $\alpha_{1C}\beta_{2a}$ (IC_{50} = 1.8 mM, n = 0.63; IC_{50} = 14.5 mM, n = 0.56, respectively) and $\alpha_{1C}\beta_{2a}\alpha_2/\delta$ (IC_{50} = 0.74, n = 1.05; IC_{50} = 1.36 mM, n = 1.8, respectively) (see text).

gered by +10-mV depolarizations were studied because this depolarization is near the maximum of both I-V relations and both measures show little voltage dependence between +10 and +30 mV (see Results, Halothane Effects on Current– and Conductance–Voltage Relations). Halothane (1 mM) reversibly depressed I_{peak} and altered the time course of currents elicited from individual cells expressing $\alpha_{1C}\beta_{2a}$ and $\alpha_{1C}\beta_{2a}\alpha_2/\delta_1$ channels (fig. 2A, top). The magnitude of I_{peak} depression was confirmed in grouped data and over a range of halothane concentrations (fig. 2B, left). Responses normalized to I_{peak} show that inactivation is enhanced by halothane for both channels, although it seemed greater with coexpression of α_2/δ_1 (fig. 2A, bottom). The magnitude of I_{300} is influenced by changes in I_{peak}, and therefore, I_{300} was plotted after normalization for I_{peak} (I_{300}/I_{peak}; fig. 2B, right). These relations show that effects on inactivation of $\alpha_{1C}\beta_{2a}\alpha_2/\delta_1$ are markedly greater than $\alpha_{1C}\beta_{2a}$ as shown by more than 10-fold difference in IC_{50} (1.38 and 14.5 mM, respectively). The results confirm halothane enhancement of inactivation for both channels and potentiation of this effect in the presence of α_2/δ subunit. Both I_{peak} and I_{300} relations show greater halothane sensitivity in the presence of α_2/δ_1. This suggests that α_2/δ_1 not only enhances control inactivation but also potentiates halothane inhibition of I_{peak}. Overall, the results suggest that phenotypic changes associated with α_2/δ_1 coexpression potentiate halothane effects on I_{peak} and apparent inactivation and are consistent with the view that voltage-dependent inactivation is a target of VA action.

Halothane Depression of Transmembrane Charge Transfer and Mean Open Probability Arise from I_{peak} Reduction

Reductions in cellular Ca^{2+} entry representing transmembrane charge transfer produced by VA inhibition of

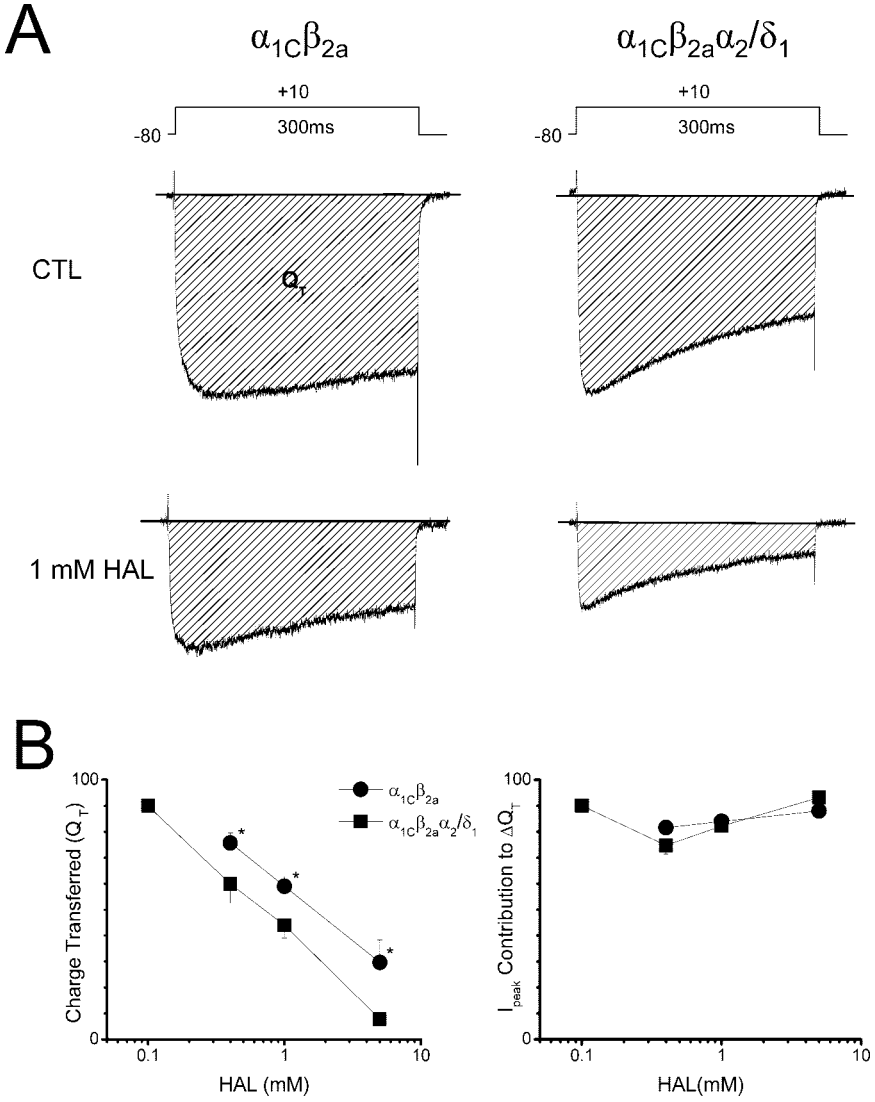

Fig. 3. Contribution of changes in peak current (I_{peak}) and current time course to depression of transmembrane charge transfer (Q_T) by halothane. (*A*) Representative current responses in control (CTL) and 1 mM halothane (HAL) to the voltage protocol shown above elicited from a single cells expressing $\alpha_{1C}\beta_{2a}$ and $\alpha_{1C}\beta_{2a}\alpha_2/\delta_1$ channels. *Solid lines* indicate baselines. *Shaded areas* under the response time course indicate the integral of current which represents the Q_T. (*B*) Plots of Q_T (percent control) and the contribution of I_{peak} (percent) to changes in charge reduction (ΔQ_T) *versus* halothane concentration in grouped data (mean ± SEM, n = 3–5 cells) for both channels as indicated (see text). * Significant differences ($P < 0.05$), unpaired *t* test.

LCCs leads to depressed cardiac contractility.[1–4] Transmembrane charge transfer is determined by current magnitude (I_{peak}) and time course (gating kinetics), which are both affected by halothane (fig. 2). We investigated the impact of changes in I_{peak} and kinetics on computed transmembrane charge transfer (Q_T; see *Methods*) to gain insight into their relative contributions (fig. 3) to reductions in cardiac contractile state. Figure 3A shows representative current responses for both channels where the charge transferred (Q_T) during a triggering stimulus is proportional to the area under the current time course (hatched area). Halothane (1 mM) markedly reduced Q_T in both channels. Charge transferred (Q_T) was steeply dependent on halothane concentration for both channels (fig. 3B, left). Approximately 1½ minimum alveolar concentration (MAC) (approximately 0.6 mM) of halothane depressed Q_T by nearly 50% in $\alpha_{1C}\beta_{2a}\alpha_2/\delta_1$ channels, whereas a similar effect in $\alpha_{1C}\beta_{2a}$ channels required more than threefold greater halothane concentration (> 2 mM). Changes in I_{peak} accounted for more than 75% of the change in Q_T over the entire concentration range, whereas halothane effects on gating (acceleration of activation and inactivation) contributed less than 25% for both channels (fig. 3B, right). This is consistent with the crudely similar current time courses in control and halothane evident after normalization for I_{peak} (fig. 2A, bottom). The similarity of I_{peak} relations despite clear differences in inactivation kinetics between these channels strongly supports a primary role of I_{peak} in determining charge transfer. Q_T was computed over a period of constant membrane potential (+10 mV, 300 ms). Mean open channel probability is proportional to Q_T, because macroscopic current is the product of single channel open probability, channel number, and unitary current that is unaltered by halothane.[5] Therefore, from this analysis, halothane depression of I_{peak} plays a primary role in the reduction of Q_T and mean open probability and likely plays an important role in LCC-mediated depression of cardiac contractility. Notably, halothane effects on channel gating (activation

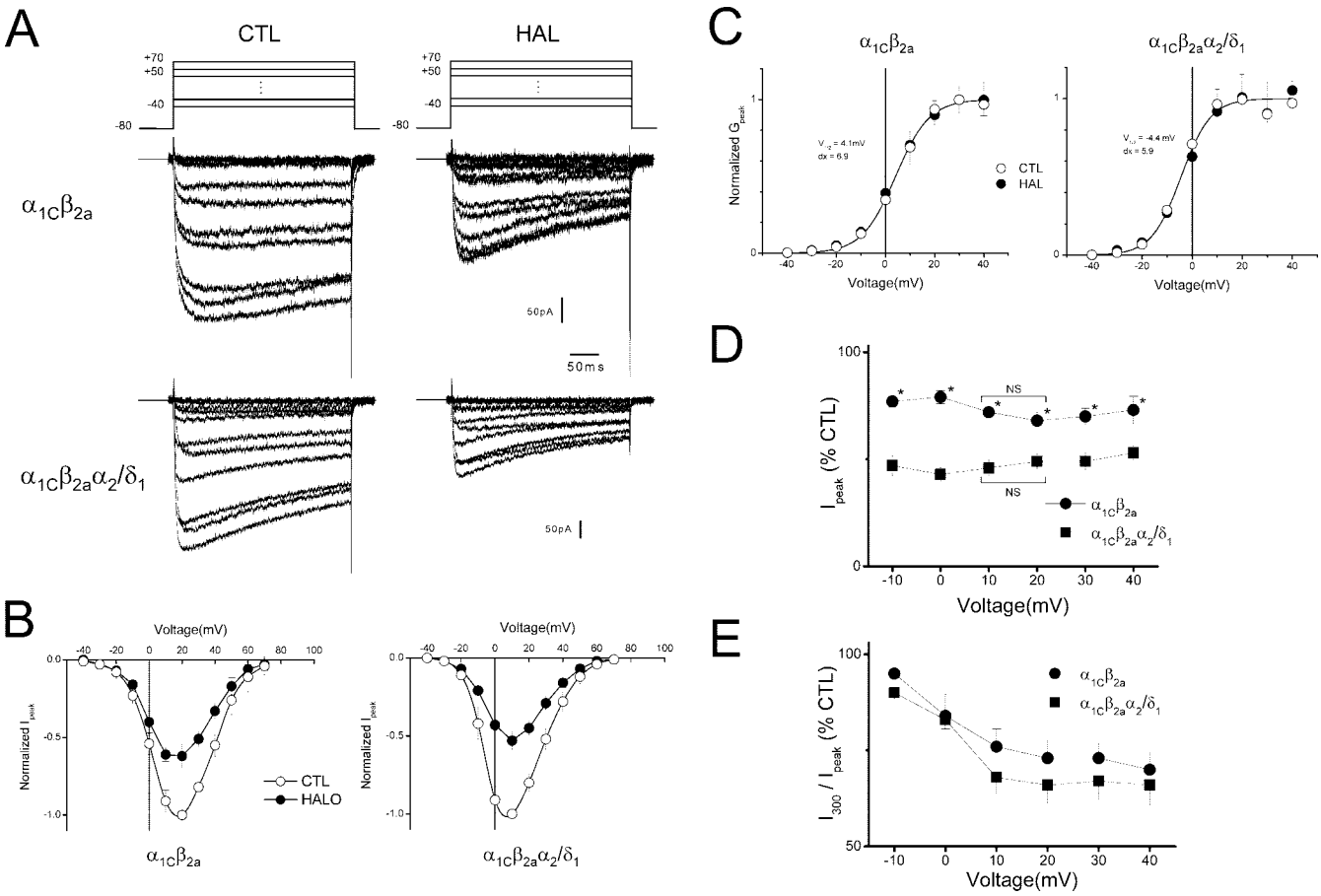

Fig. 4. Halothane effects on current–voltage relations and activation of $\alpha_{1C}\beta_{2a}$ and $\alpha_{1C}\beta_{2a}\alpha_2/\delta$ channels. (*A*) Representative current–voltage families triggered by voltage steps (−40 to +70mV, 300 ms, 10-mV increments, holding potential −80 mV as drawn above) for HEK-293 cells expressing $\alpha_{1C\beta 2a}$ (*top*) and $\alpha_{1C}\beta_{2a}\alpha_2/\delta$ (*bottom*) subunits in control (CTL) and in 1 mM halothane (HAL). Control families replotted from figure 1A for comparison. (*B*) Normalized mean current–voltage relations for $\alpha_{1C}\beta_{2a}$ (*left*) and $\alpha_{1C}\beta_{2a}\alpha_2/\delta$ (*right*) in control (CTL) and in halothane (HALO) (1 mM) (mean ± SEM, n = 4 or 5 cells). (*C*) Normalized peak conductance (G_{peak}), as computed from peak current (I_{peak}) and reversal potential (see Materials and Methods) *versus* triggering voltage for both channels in control (○) and 1 mM halothane (●) from grouped data (mean ± SEM, n = 4–6) as indicated. *Solid line* represents overall Boltzmann function fit (see Materials and Methods) of both relations, with fitted parameters as indicated. (*D*) Voltage dependence of I_{peak} depression (percent of control) by 1 mM halothane for both channels as indicated. NS = not significant paired *t* test. * Significant differences ($P < 0.05$, unpaired *t* test). (*E*) Voltage dependence of normalized magnitude of enhanced inactivation (I_{300}/I_{peak}, percent of control) produced by 1 mM halothane for both channels as indicated.

and inactivation) make minor contributions to reductions in Q_T and mean open probability. The results point to the importance of halothane interactions with channel states present at resting membrane potentials, which may underlie reductions in I_{peak}.

Halothane Effects on Current- and Conductance–Voltage Relations

We next examined halothane effects on channel function over a range of triggering potentials. Figure 4A shows families of current responses triggered over a range of triggering potentials in control and 1 mM halothane for both channel types. Inspection of resultant I-V relations indicates that halothane depressed I_{peak} values without apparent changes in the nature of these relations (fig. 4B). This indicates that halothane reduced the number channels available to activate during a triggering depolarization. Halothane reduces time to peak (see Results, Halothane Alters Activation and Inactivation Kinetics), which may be explained by acceleration of activation; we therefore first investigated the voltage dependence of activation by constructing peak conductance (G_{peak})–voltage relations. G_{peak} reports the peak channel open probability. G_{peak} was computed from peak ionic current measurements and the driving force as determined from the difference between test voltage and measured reversal potential (see Materials and Methods). For each channel type, after normalization for maximum G_{peak}, control and halothane relations show a similar dependence on voltage, indicating that the voltage dependence of peak open probability is unaltered by halothane (fig. 4C). To further investigate the effects of halothane on the number of activatable channels, we examined the voltage dependence of halothane depression of I_{peak} (fig. 4D). In channels with and without the α_2/δ_1 subunit, halothane's

effect showed little voltage dependence, consistent with halothane's primary effect of alteration in the number of activatable channels. Statistical means testing demonstrated no detectable difference in this endpoint between 10- and 20-mV triggering potentials for each channel type. The magnitude of apparent inactivation enhancement (300-ms depolarizations) produced by halothane was potentiated by increasing depolarization until reaching a seeming plateau at approximately 10 mV for both channels (fig. 4E).

Halothane Alters Activation and Inactivation Kinetics

Normalized current traces indicate that halothane reduced the time to I_{peak} for both channels (fig. 2A, bottom, insets). Time to I_{peak}, determined by inspection, was reduced by halothane for $\alpha_{1C}\beta_{2a}$ (control, 54.8 ± 6.9 ms; halothane, 37.0 ± 4.3 ms; $P < 0.01$) and $\alpha_{1C}\beta_{2a}\alpha_2/\delta_1$ (control, 21.8 ± 3.7 ms; halothane, 14.1 ± 2.3 ms; $P < 0.01$). G_{peak} reflects peak open channel probability, and time to peak of macroscopic current reports the time point of this event, presuming that unitary conductance remains constant. Both measures are primarily dependent on channel opening and activation and are opposed by channel closure, deactivation, and inactivation. As a result, it is notable that halothane reduced time to I_{peak} unaccompanied by changes in the form of the conductance–voltage relation. We therefore were interested in determining the effects of halothane on channel activation and inactivation through the quantitative analysis of the current time course. Current time courses were fitted with multiexponential functions, which provides for the separation and quantitation of activation and inactivation kinetics (see Materials and Methods). The $\alpha_{1C}\beta_{2a}$ current time course was well fit by a triexponential function (equation 3), where activation was described by two exponential components (time constants: fast [τ_f] and slow [τ_s]) and inactivation by single component (time constant: τ_i) (fig. 5A). Both components of activation were accelerated by halothane (fig. 5B) without changes in relative proportion (fig. 5B, bottom left). Halothane also accelerated inactivation (fig. 5B, bottom right). These effects were generally observed over a range of triggering voltages.

The time course of currents carried by $\alpha_{1C}\beta_{2a}\alpha_2/\delta_1$ were also well fit by a triexponential function (equation 3) but with monoexponential activation (time constant: τ_a) and biexponential inactivation (time constants: τ_s and τ_f) (fig. 6A), consistent with previous reports.[16] Both activation and inactivation were accelerated by halothane (fig. 6B). We next investigated the effects of triggering voltages on halothane acceleration of activation and inactivation. Halothane acceleration of activation was present throughout the voltage range, although this affect appeared less at greater depolarizations (fig. 6B, top left). Overall, inactivation was accelerated through the reduction of time constants for both components at triggering voltages of 0 and 10 mV and enhancement of the fast fraction at 10 to 30 mV (fig. 6B). Finally, halothane effects on both components of $\alpha_{1C}\beta_{2a}\alpha_2/\delta_1$ inactivation were enhanced by concentration (fig. 6C).

Discussion

The results demonstrate that halothane differentially modulated currents through recombinant LCCs with divergent gating characteristics determined by α_2/δ_1 coexpression. Halothane depressed I_{peak} and enhanced apparent inactivation for both channels. The magnitude of these effects was markedly greater with coexpression of α_2/δ_1 subunit, which also enhanced voltage-dependent inactivation. A central result is that halothane depression of transmembrane charge transfer and mean open probability is primarily governed by reductions in I_{peak} and not by changes in current time course (activation and inactivation). Furthermore, depression of I_{peak} arises from channel transitions to nonactivatable states occurring at resting membrane potential or early in the activation cascade. The findings provide strong evidence for the hypothesis that the phenotypic differences associated with the changes in voltage-dependent inactivation play key roles in the mechanism of inhibition of LCCs by halothane. However, it remains unclear as to whether the important effects of halothane on I_{peak} arise from differences in voltage-dependent inactivation or other attendant but unrecognized changes in phenotype resulting from α_2/δ_1 coexpression. Overall, these results set the stage for studies to elucidate critical channel structures involved in the halothane inhibition of cardiac LCCs and to provide a deeper understanding of the inhibitory mechanism.

Coexpression of α_2/δ_1 Potentiates Inactivation and Halothane Inhibition of I_{peak}

Coexpression of α_2/δ_1 subunit with the pore-forming α subunit and accessory β subunit enhances macroscopic inactivation.[17,19] As a result, we studied channels arising from α_{1C} and β_{2a} subunits coexpressed with and without the α_2/δ_1 subunit. Coexpression of α_2/δ_1 subunit resulted in macroscopic currents with enhanced inactivation, and leftward shifts of I-V and conductance–voltage relations consistent with previous reports.[16] Reproduction of these features also supports the position that green fluorescent protein tagging of the α_{1C} subunit does not alter fundamental channel function.[19] Halothane produced reversible, concentration-dependent depression of I_{peak} for both channels (fig. 2). Concentration–response relations for I_{peak} are reported for a triggering potential of 10 mV, at which the halothane effects on these endpoints reached a plateau as a func-

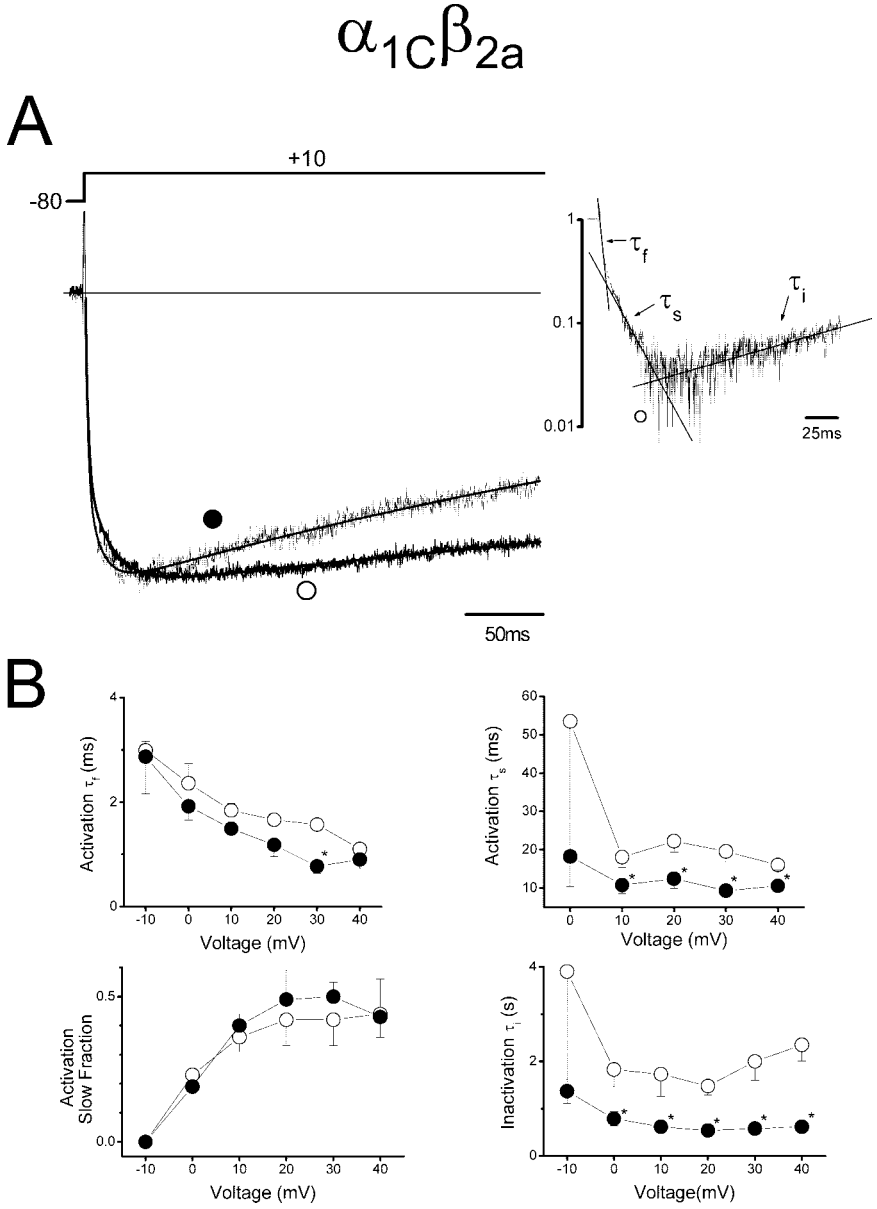

Fig. 5. Halothane effects on the voltage dependence of the $\alpha_{1C}\beta_{2a}$ current time course. (*A*) Currents from an individual cell expressing $\alpha_{1C}\beta_{2a}$ channels replotted on an expanded timescale from figure 2A in control (○) and 1 mM halothane (●) triggered by a voltage step (+10 mV, 300 ms, holding potential −80 mV as drawn here). *Solid lines* are the best fit of a triexponential function (equation 3, see Materials and Methods). (*Inset*) Control response replotted on semilogarithmic axes to demonstrate exponential components of activation (fast [τ_f] and slow [τ_s]) and inactivation (τ_i). *Thin lines* represent time course of the indicated single exponential components. (*B*) Voltage dependence of fitted exponential parameters for activation (τ_f [*top left*] and τ_s [*top right*]) and inactivation (τ_i [*bottom right*]), as well as percentage of the activation that is slow (slow fraction [*bottom left*]) in control (○) and 1 mM halothane (●) in grouped data (mean ± SEM, n = 4–6). * Significant differences between control and halothane ($P < 0.05$, paired *t* test).

tion of activating voltage (fig. 4D), suggesting that differences in activation did not contribute to the findings.

$\alpha_{1C}\beta_{2a}\alpha_2/\delta_1$ likely reflects the function of *in vivo* channels.[14] Therefore, it is reasonable to compare the $\alpha_{1C}\beta_{2a}\alpha_2/\delta_1$ results from this study with those reported for native LCCs. Halothane (0.4 mM) depressed I_{peak} of $\alpha_{1C}\beta_{2a}\alpha_2/\delta_1$ by 34%, which is roughly comparable to the 25–45% I_{peak} reduction reported for native LCCs with Ba^{2+} as the charge carrier: I_{peak} was reduced 25% by 0.45 mM halothane in guinea pig ventricular myocytes,[5] by 35% with 0.4 mM halothane in canine ventricular myocytes,[22] by 35% with 0.45 mM halothane in canine cardiac Purkinje cells,[23] and by 25% with 0.41 mM halothane in neuronal SH-SY5Y cells.[7] Similar results have been reported with recombinant $\alpha_{1C}\beta_{2b}\alpha_2/\delta_1$ channels expressed in *Xenopus* oocytes, where 0.59 mM halothane depressed I_{peak} by 45%.[8]

The results of the current study suggest that halothane depresses I_{peak} through the reduction of activatable channels at resting membrane potentials. However, the underlying mechanism remains unclear but may be explained by a hyperpolarizing shift in the steady state inactivation. Isoflurane has been reported to produce significant shifts in the steady state inactivation curve in recombinant $\alpha_{1E}\beta_{2b}\alpha_2/\delta_1$ [8] and in native LCCs in cardiac and nervous tissue.[5,24–27] However, such shifts have not been reported with halothane in native cardiac[5,28] or recombinant LCCs,[8] pointing to possible divergent effects of these volatile agents on LCC function.[29] Examination of steady state inactivation was beyond the scope of the current study. Interestingly, single-channel studies have demonstrated that halothane significantly increases the fraction of null sweeps and the duration of sojourns into nonconducting states.[5,7] In the absence of hyperpo-

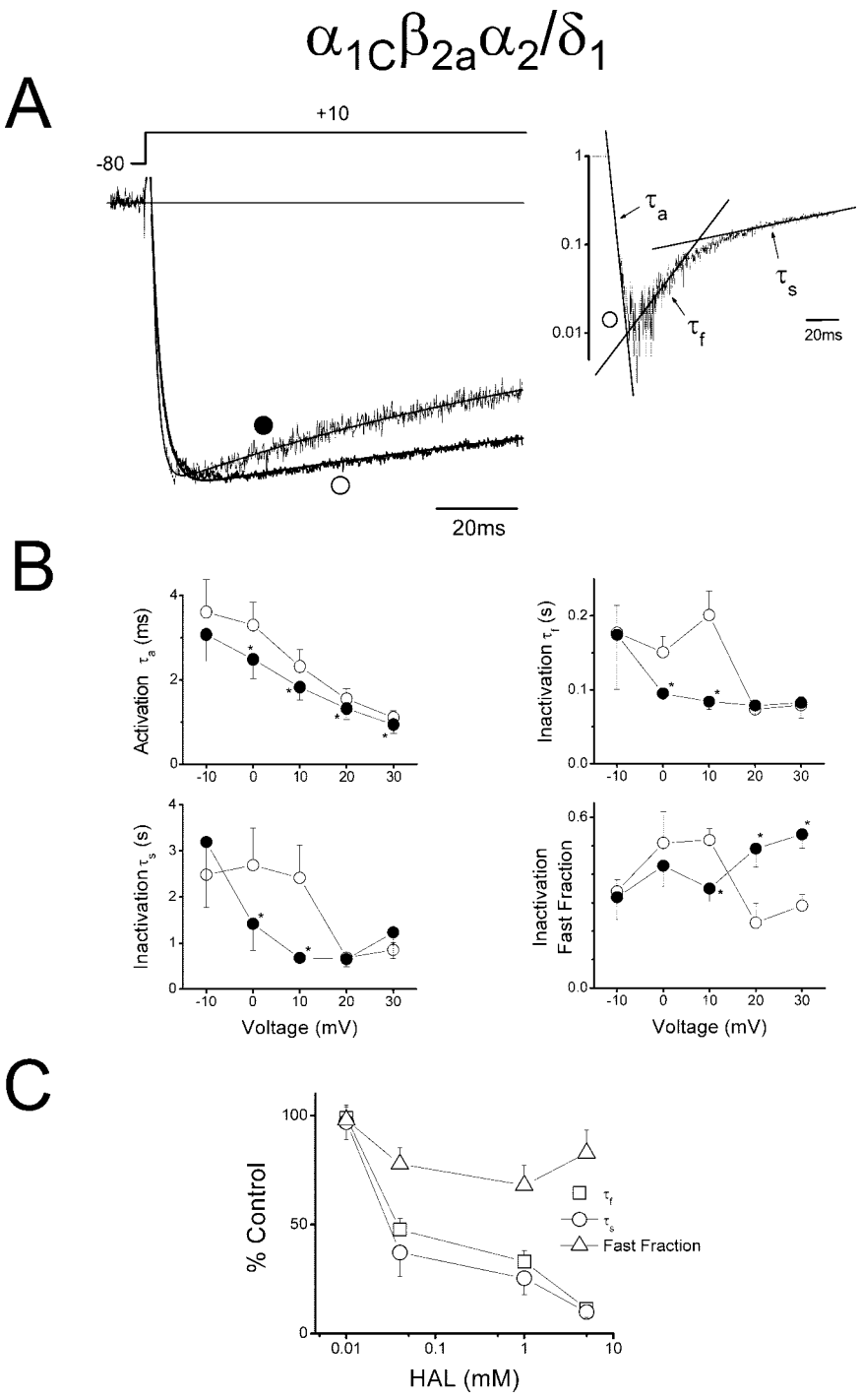

Fig. 6. Halothane effects on the voltage dependence of the $\alpha_{1C}\beta_{2a}\alpha_2/\delta_1$ current time course. (*A*) Currents from an individual cell expressing $\alpha_{1C}\beta_{2a}\alpha_2/\delta_1$ channels replotted on an expanded timescale from figure 2A in control (○) and 1 mM halothane (●) triggered by a voltage step (+10 mV, 300 ms, holding potential −80 mV as drawn here). *Solid lines* are the best fit of a triexponential function (equation 2, see Materials and Methods). (*Inset*) Control response replotted on semilogarithmic axes to demonstrate exponential components of activation (τ_a) and fast (τ_f) and slow (τ_s) inactivation. *Thin lines* represent time course of the indicated single exponential components. Capacity currents clipped for purposes of display. (*B*) Voltage dependence of fitted parameters for τ_a (*top left*), τ_f (*top right*), and τ_s (*bottom left*), and fraction of inactivation that is fast (*bottom right*) in control (○) and 1 mM halothane (●) in grouped data (mean ± SEM, n = 4–6). * Significant differences between control and halothane ($P < 0.05$, paired *t* test). (*C*) Fitted exponential inactivation parameters in halothane (HAL) normalized to control and plotted *versus* halothane concentration.

larizing shifts of steady state inactivation, these single-channel results in combination with unaltered macroscopic activation suggest that halothane depresses I_{peak} by promoting transitions from resting to drug-induced nonactivatable states as suggested by Pancrazio.[5] Overall, we interpret these findings as support for distinct but overlapping mechanisms of LCC inhibition by halothane and isoflurane as suggested previously.[1,5,30] This concept is consistent with the structural diversity of these compounds that gives rise to marked differences in molecular polarity.[31]

Changes in I_{peak} Determine Reductions in Charge Transfer and Mean Open Probability Produced by Halothane

Reductions in Ca^{2+} entry through LCCs contribute importantly to halothane depression of the contractile state of the heart. To gain insight into halothane-mediated depression of Ca^{2+} entry, we computed charge transfer (Q_T) triggered by depolarizations (+10 mV, 300 ms) that roughly approximate the magnitude and duration of a cardiac action potential. Q_T is also proportional to mean open probability. The results indicate that

changes in I_{peak} are the primary determinant of charge entry through LCCs with halothane. Halothane produced enhancement of inactivation during a triggering depolarization. However, the resultant current decrease due to inactivation contributed little to the reduction of Q_T and mean open probability relative to the effects of I_{peak}. It is possible that *in vivo*, the impact of reductions in I_{peak} could be magnified because inhibition of LCCs causes cardiac action potential shortening,[32] which itself leads to additional decrease in Ca^{2+} entry. The results should be interpreted with some caution because Ba^{2+} was used as the charge carrier in this study. Reduction of I_{peak} was significantly greater for Ba^{2+} *versus* Ca^{2+} as the charge carrier (68 and 57%, respectively), but only at highest halothane concentration (1.8 mM) in cardiac myocytes.[5] Overall, the results suggest that with regard to cardiac contractility, an important effect of halothane is depression of Ca^{2+} entry into cardiac myocytes through reduction of I_{peak}. Rapid activation relative to inactivation and conductance–voltage relations unchanged by halothane argue for the involvement of channels states present at resting membrane potentials in the mechanism of halothane depression of I_{peak} but do not rule out the involvement of states visited early in activation.

Coexpression of α_2/δ_1 Potentiates Inactivation and Enhancement by Halothane

Coexpression of α_2/δ_1 subunit enhanced inactivation as well as increased sensitivity to the effects of halothane on inactivation (fig. 2B). Divergent concentration–response relations in magnitude of inactivation (I_{300}/I_{peak}) for the two types of channels were obtained using a triggering potential of +10 mV. Halothane effects on inactivation reached an apparent plateau at a triggering potential of +10 mV (figs. 4E, 5B, and 6B) despite distinctive voltage dependent gating for both of these two channels types (fig. 1). Therefore, such dissimilarities in native gating of these channels are unlikely to contribute to the differences in halothane effects.

In the current study, Ba^{2+} was the charge carrier, and pipette solutions included a Ca^{2+} chelator, which minimized contributions by Ca^{2+}-mediated current inactivation. Therefore, current inactivation is primarily due to a voltage-dependent process rather one triggered by Ca^{2+}. Overall, these findings are interpreted to indicate that molecular transitions and or channel states involved in voltage-dependent inactivation play a role in the pharmacologic action of halothane as suggested by Pancrazio[5] and has also been proposed for isoflurane.[6] However, the above result strongly points to the possibility that unrecognized phenotypic changes associated with altered inactivation as induced by coexpression of α_2/δ_1 may be importantly involved in the action of halothane. Possible phenotypic changes may include fundamental changes in binding site affinity or accessibility, or changes in the allosteric effects of binding site occupation independent of affinity changes, for example. Finally, the results suggest that the contribution of changes in apparent macroscopic inactivation assumes a role secondary to changes in I_{peak} in reducing Ca^{2+} entry.

Voltage-dependent inactivation is a prominent feature of α_{1C} and L-type calcium channels. Halothane increases the magnitude of inactivation and the apparent inactivation rate observed during 300-ms depolarizations. These effects were greater when accompanied by enhanced intrinsic voltage-dependent inactivation produced by coexpression with α_2/δ_1 (figs. 2, 5, and 6). For $\alpha_{1C}\beta_{2a}\alpha_2/\delta_1$ channels, 0.4 mM halothane produced roughly similar current reductions with 300 ms of depolarization in guinea pig myocytes[5] and neuronal SH-SY5Y cells[7] with Ba^{2+} as the charge carrier. Halothane did not enhance inactivation in recombinant $\alpha_{1C}\beta_{2b}\alpha_2/\delta_1$ channels expressed in *Xenopus* oocytes.[8] However, these channels also showed little inactivation in control conditions, which may be attributed to the heterologous expression system or accessory subunit subtypes. When Ca^{2+} is the charge carrier, halothane also enhanced inactivation in CA1 neurons[33] and GH3 cells,[34] which may also involve effects on Ca^{2+}-mediated inactivation. However, Fassl[35] investigated the effect of halothane on LCCs in human atrial cells and found slowing of inactivation at approximately 2 MAC. This latter result may reflect species or preparation differences or genuine divergence between atrial and ventricular channels to the effects of VA.[27]

Halothane Accelerates Activation

Halothane reduces the time to I_{peak} for both channels, which is accompanied by acceleration of macroscopic activation. The results are consistent with those in adrenal chromaffin cells,[36] where 1.4 mM halothane decreased LCC calcium currents by approximately 30% and enhanced activation rate with no change in the voltage dependence of peak conductance. Overall, these observations may be explained by rapid activation relative to inactivation in combination with commensurate halothane-induced increases in microscopic activation and deactivation rates such that voltage dependence of peak open probability is unaltered. In contrast, halothane slowed activation in cultured neuronal SH-SY5Y cells[7] and had no effect in rat sensory neurons[37] and GH3 pituitary cells.[34] These findings point to pharmacologic differences among these LCCs derived from different cells and preparations.

Halothane Acceleration of $\alpha_{1C}\beta_{2a}\alpha_2/\delta_1$ Inactivation Kinetics Is Voltage Dependent

To explore for possible state dependence of LCC inhibition, we investigated the voltage dependence of halothane acceleration of inactivation. Triggering voltage determines peak open probability as reported by conductance–voltage relations (fig. 4). To gain insight into the involvement of states associated with channel

activation (open and inactivated), we investigated changes in current time course over a range of triggering potentials. Halothane accelerated inactivation kinetics of $\alpha_{1C}\beta_{2a}$ channels, but with little voltage dependence (fig. 5B). Both components of $\alpha_{1C}\beta_{2a}\alpha_2/\delta_1$ inactivation were accelerated by triggering voltages ranging from 0 to +10 mV, whereas fast fraction was enhanced at voltages exceeding 10 mV (fig. 6). The results suggest that halothane acts on open and inactivated states of $\alpha_{1C}\beta_{2a}\alpha_2/\delta_1$ by either promotion of these states, leading to inactivation or direct inhibition.

The authors thank Robert Kass, Ph.D. (Professor of Pharmacology, Columbia University, New York, New York), for rabbit skeletal muscle α_2/δ_1 and heart β_{2a} and Robert Dirksen, Ph.D. (Associate Professor of Pharmacology and Physiology, University of Rochester, Rochester, New York), for α_{1C} tagged with green fluorescent protein.

References

1. Lynch C III, Vogel S, Sperelakis N: Halothane depression of myocardial slow action potentials. ANESTHESIOLOGY 1981; 55:360–8
2. Bosnjak ZJ, Aggarwal A, Turner LA, Kampine JM, Kampine JP: Differential effects of halothane, enflurane, and isoflurane on Ca^{2+} transients and papillary muscle tension in guinea pigs. ANESTHESIOLOGY 1992; 76:123–31
3. Schmidt U, Schwinger RH, Bohm S, Uberfuhr P, Kreuzer E, Reichart B, Meyer L, Erdmann E, Bohm M: Evidence for an interaction of halothane with the L-type Ca^{2+} channel in human myocardium. ANESTHESIOLOGY 1993; 79:332–9
4. Blanck TJ, Lee DL, Yasukochi S, Hollmann C, Zhang J: The role of L-type voltage-dependent calcium channels in anesthetic depression of contractility. Adv Pharmacol 1994; 31:207–14
5. Pancrazio JJ: Halothane and isoflurane preferentially depress a slowly inactivating component of Ca^{2+} channel current in guinea-pig myocytes. J Physiol 1996; 494:91–103
6. Hirota K, Fujimura J, Wakasugi M, Ito Y: Isoflurane and sevoflurane modulate inactivation kinetics of Ca^{2+} currents in single bullfrog atrial myocytes. ANESTHESIOLOGY 1996; 84:377–83
7. Nikonorov IM, Blanck TJ, Recio-Pinto E: The effects of halothane on single human neuronal L-type calcium channels. Anesth Analg 1998; 86:885–95
8. Kamatchi GL, Chan CK, Durieux ME, Snutch TP, Lynch C III: Volatile anesthetic inhibition of neuronal Ca^{2+} channel currents expressed in Xenopus oocytes. Brain Res 1999; 831: 85–96
9. Yamakage M, Namiki A: Calcium channels–basic aspects of their structure, function and gene encoding: Anesthetic action on the channels—a review. Can J Anaesth 2002; 49:151–64
10. Huneke R, Fassl J, Rossaint R, Luckhoff A: Effects of volatile anesthetics on cardiac ion channels. Acta Anaesthesiol Scand 2004; 48:547–61
11. Armstrong CM: Interaction of tetraethylammonium ion derivatives with the potassium channels of giant axons. J Gen Physiol 1971; 58:413–37
12. Hille B: Local anesthetics: Hydrophilic and hydrophobic pathways for the drug-receptor reaction. J Gen Physiol 1977; 69:497–515
13. Cai D, Mulle JG, Yue DT: Inhibition of recombinant Ca^{2+} channels by benzothiazepines and phenylalkylamines: Class-specific pharmacology and underlying molecular determinants. Mol Pharmacol 1997; 51:872–81
14. Catterall WA: Structure and regulation of voltage-gated Ca^{2+} channels. Annu Rev Cell Dev Biol 2000; 16:521–55
15. Stotz SC, Zamponi GW: Structural determinants of fast inactivation of high voltage-activated Ca^{2+} channels. Trends Neurosci 2001; 24:176–81
16. Klugbauer N, Lacinova L, Marais E, Hobom M, Hofmann F: Molecular diversity of the calcium channel $\alpha_2\delta$ subunit. J Neurosci 1999; 19:684–91
17. Arikkath J, Campbell KP: Auxiliary subunits: Essential components of the voltage-gated calcium channel complex. Curr Opin Neurobiol 2003; 13:298–307
18. Dhallan RS, Yau KW, Schrader KA, Reed RR: Primary structure and functional expression of a cyclic nucleotide-activated channel from olfactory neurons. Nature 1990; 347:184–7
19. Grabner M, Dirksen RT, Beam KG: Tagging with green fluorescent protein reveals a distinct subcellular distribution of L-type and non-L-type Ca^{2+} channels expressed in dysgenic myotubes. Proc Natl Acad Sci U S A 1998; 95:1903–8
20. Ferreira G, Yi J, Rios E, Shirokov R: Ion-dependent inactivation of barium current through L-type calcium channels. J Gen Physiol 1997; 109:449–61
21. Bangalore R, Mehrke G, Gingrich K, Hofmann F, Kass RS: Influence of L-type Ca^{2+} channel alpha 2/delta-subunit on ionic and gating current in transiently transfected HEK 293 cells. Am J Physiol 1996; 270:H1521–8
22. Bosnjak ZJ, Supan FD, Rusch NJ: The effects of halothane, enflurane, and isoflurane on calcium current in isolated canine ventricular cells. ANESTHESIOLOGY 1991; 74:340–5
23. Eskinder H, Rusch NJ, Supan FD, Kampine JP, Bosnjak ZJ: The effects of volatile anesthetics on L- and T-type calcium channel currents in canine cardiac Purkinje cells. ANESTHESIOLOGY 1991; 74:919–26
24. Park WK, Pancrazio JJ, Suh CK, Lynch C III: Myocardial depressant effects of sevoflurane: Mechanical and electrophysiologic actions in vitro. ANESTHESIOLOGY 1996; 84: 1166–76
25. Wilde DW: Isoflurane reduces K+ current in single smooth muscle cells of guinea pig portal vein. Anesth Analg 1996; 83:1307–13
26. Kameyama K, Aono K, Kitamura K: Isoflurane inhibits neuronal Ca^{2+} channels through enhancement of current inactivation. Br J Anaesth 1999; 82:402–11
27. Camara AK, Begic Z, Kwok WM, Bosnjak ZJ: Differential modulation of the cardiac L- and T-type calcium channel currents by isoflurane. ANESTHESIOLOGY 2001; 95:515–24
28. Niggli E, Rudisuli A, Maurer P, Weingart R: Effects of general anesthetics on current flow across membranes in guinea pig myocytes. Am J Physiol 1989; 256:C273–81
29. Baum VC, Wetzel GT, Klitzner TS: Effects of halothane and ketamine on activation and inactivation of myocardial calcium current. J Cardiovasc Pharmacol 1994; 23:799–805
30. Terrar DA, Victory JG: Effects of halothane on membrane currents associated with contraction in single myocytes isolated from guinea-pig ventricle. Br J Pharmacol 1988; 94:500–8
31. Cafiso DS: Dipole potentials and spontaneous curvature: Membrane properties that could mediate anesthesia. Toxicol Lett 1998; 100–101: 431–9
32. Suzuki A, Aizawa K, Gassmayr S, Bosnjak ZJ, Kwok WM: Biphasic effects of isoflurane on the cardiac action potential: An ionic basis for anesthetic-induced changes in cardiac electrophysiology. ANESTHESIOLOGY 2002; 97:1209–17
33. Krnjevic K, Puil E: Halothane suppresses slow inward currents in hippocampal slices. Can J Physiol Pharmacol 1988; 66:1570–5
34. Herrington J, Stern RC, Evers AS, Lingle CJ: Halothane inhibits two components of calcium current in clonal (GH3) pituitary cells. J Neurosci 1991; 11:2226–40
35. Fassl J, Halaszovich CR, Huneke R, Jungling E, Rossaint R, Luckhoff A: Effects of inhalational anesthetics on L-type Ca^{2+} currents in human atrial cardiomyocytes during β-adrenergic stimulation. ANESTHESIOLOGY 2003; 99:90–6
36. Pancrazio JJ, Park WK, Lynch C III: Inhalational anesthetic actions on voltage-gated ion currents of bovine adrenal chromaffin cells. Mol Pharmacol 1993; 43: 783–94
37. Takenoshita M, Steinbach JH: Halothane blocks low-voltage-activated calcium current in rat sensory neurons. J Neurosci 1991; 11:1404–12